Cyclotron-resonance studies in relaxed $In_xGa_{1-x}As$ ($0 \leq x \leq 1$) epilayers

J. L. Shen, Y. D. Dai, and Y. F. Chen
Physics Department, National Taiwan University, Taipei, Taiwan, Republic of China

S. Z. Chang and S. C. Lee
Electrical Engineering Department, National Taiwan University, Taipei, Taiwan, Republic of China
(Received 30 December 1994)

By the techniques of far-infrared optically detected cyclotron resonance and magnetophotoconductivity, we have performed cyclotron-resonance measurements on relaxed $In_xGa_{1-x}As$ epitaxial layers with a wide range of composition. The measured electron effective mass as a function of indium composition has been analyzed with the five-band $\mathbf{k}\cdot\mathbf{p}$ calculation. It is found that the effect of disorder-induced conduction–valence-band mixing must be included in order to resolve the discrepancy between the results of the $\mathbf{k}\cdot\mathbf{p}$ theory and experiments. The linewidths of cyclotron resonance and photoluminescence as a function of alloy composition have also been studied. Comparing with the measurement of double-crystal x-ray diffraction, we point out that the cyclotron-resonance and photoluminescence signals in $In_xGa_{1-x}As$ alloys are dominated by the dislocation scattering. In addition, we show that the quality of a ternary epilayer is not only influenced by the lattice mismatch; the surface migration lengths of the cation atoms in the initial growth stage also play a very important role.

I. INTRODUCTION

The ternary alloy semiconductor $In_xGa_{1-x}As$ has been of great interest due to its potentiality in the construction of electronic and optoelectronic devices. As a result, the physical properties of this material system have received attention in recent decades. The experimental determination of the electron effective mass in $In_xGa_{1-x}As$ alloys was made in the 1960s.[1–3] However, because the effective masses were obtained by indirect methods (e.g., the plasma-edge reflection or the Faraday rotation), the accuracy of these results is doubtful.[4,5] (1) Since the studied samples were mostly n-type heavily doped, the results did not clearly yield the effective mass at the bottom of the conduction band. (2) The interpretation requires the actual values of other physical properties such as the index of refraction or the room-temperature band gap, which were not very reliable at that time. Later, precise measurement using the conventional electron cyclotron-resonance (CR) was reported by Fetterman, Waldman, and Wolfe.[4] However, their data were only limited to a small range of alloy composition ($0 \leq x \leq 0.154$). To the best of our knowledge, a complete and accurate measurement of the electron effective mass in $In_xGa_{1-x}As$ alloys with a wide range of composition ($0 \leq x \leq 1$) has not been reported.

Here we present CR studies in a series of $In_xGa_{1-x}As$ epilayers with $0 \leq x \leq 1$. In order to carry out the measurements successfully, several considerations were made before the experiments. Firstly, to prevent the CR condition $\omega_c\tau \gg 1$ (ω_c and τ are the cyclotron frequency and the single-particle scattering time, respectively) from being violated by the misfit dislocations, the InP substrate was used for $0.48 \leq x \leq 0.73$ and GaAs for other values. Secondly, the variation of the effective mass induced by the misfit stress was avoided by keeping the thickness of the studied sample (2 μm) much larger than the critical thickness of the stress relaxation. Thirdly, it is known that the intrinsic carrier concentrations of $In_xGa_{1-x}As$ alloys are small, especially for low indium composition. The conventional CR measurement is not adequate for these samples. Our CR measurements were hence performed by using the technique of far-infrared (FIR) optically detected cyclotron resonance (ODCR) for low indium composition ($x \leq 0.66$), in which the necessary carriers are provided by optical pumping. Thus, the change of the effective mass induced by nonparabolicity can be greatly reduced. While due to the limitation of the response of our detector, the FIR-magnetophotoconductivity technique was used for the samples with high indium composition ($x > 0.66$). The obtained $In_xGa_{1-x}As$ effective mass as a function of alloy composition was compared with the five-band $k\cdot\mathbf{p}$ calculation.[5] It is found that the calculated effective masses are smaller than that of the experimental values. We point out that the conduction–valence-band mixing induced by the alloy disorder may be the possible cause for the origin of this discrepancy. We have also investigated the compositional dependence of the full width at half maximum (FWHM) of the CR and photoluminescence (PL) spectra. Comparing with the double-crystal x-ray diffraction (DXRD) measurement, we find a clear correlation of the linewidths among the DXRD, CR, and PL signals. Because the DXRD signals are very sensitive to the dislocations in the heteroepitaxial systems, we thus conclude that the CR and PL signals are dominated by the dislocation scattering. In addition, from the analysis of these FWHM's, we show that the factors affecting the quality of the relaxed $In_xGa_{1-x}As$ epilayers include lattice mismatch as well as surface migration lengths of the cation atoms in the initial growth stage.

II. EXPERIMENTAL PROCEDURE

The investigated samples were 2-μm-thick undoped $In_xGa_{1-x}As$ ($0 \leq x \leq 1$) epilayers grown in a VB V80H MK II molecular-beam-epitaxy system. Details of the growth conditions for these samples have been reported elsewhere.[6] The characteristics (composition and substrate) of the samples are listed in Table I. For the cyclotron-resonance detection, we use two different kinds of techniques for the experiments. In the ODCR measurement, resonant absorption of FIR is detected by the changes in luminescence intensity at the magnetic field corresponding to cyclotron resonance.[7–9] The sample was placed in a 7T Oxford superconducting magnet under the Faraday geometry. An Edinburgh Instruments CO_2-pumped far-infrared laser working at 118.8 μm was used to generate FIR radiation. The FIR light was guided by mirrors to the sample and was modulated by a mechanical chopper. The luminescence was excited with an Ar-ion laser, dispersed by a SPEX 0.5 m monochromator, and detected by a LN_2-cooled North Coast Ge detector. In the FIR-magnetophotoconductivity measurement, the light source and experimental configuration are the same as that of the ODCR measurement. The photoresponse was carried out in a constant-current mode and detected as a change in the voltage drop across the sample using a lock-in amplifier. The temperature was held at 5 K in all cases.

III. RESULTS AND DISCUSSION

The PL spectra of $In_xGa_{1-x}As$ alloys with the composition $x = 0.16$, 0.20, 0.39, 0.48, 0.59, and 0.66 are shown in Fig. 1. We can see that the peak energy of the spectrum decreases as the alloy composition increases. The main PL signals from these samples (except for $In_{0.39}Ga_{0.61}As$) can be attributed to the recombinations of the excitons bound to neutral impurities.[10,11] The weak

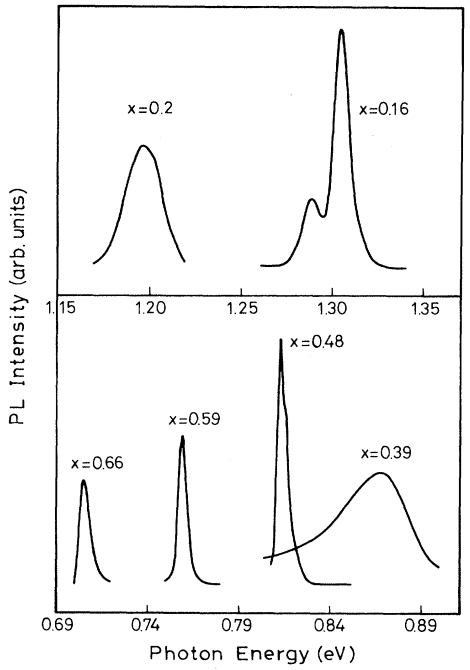

FIG. 1. PL spectra of $In_xGa_{1-x}As$ alloys at $T = 5$ K.

structure appearing at the lower energy side of the main peak in $In_{0.16}Ga_{0.84}As$ is due to a mixture of conduction-band—acceptor and donor-acceptor pair recombinations.[11] With Fig. 1, the energy band gap of the samples can be obtained from the peak position of the PL spectrum. It is known that the binding energy E_d of the donor bound exciton can be determined from the hydrogenic model:[12]

$$E_d = [(\mu/m_0)/\epsilon_0^2] \times 13.6 \text{ eV} , \quad (1)$$

where $1/\mu = 1/m_e^* + 1/2(1/m_{hh}^* + 1/m_{lh}^*)$. If we linear-

TABLE I. Values of electron effective mass, CR FWHM, energy gap E_0, PL FWHM, and DXRD FWHM for $In_xGa_{1-x}As$ alloys.

Sample	Substrate	Effective mass (m_0)	CR FWHM (T)	PL peak position (eV)	PL FWHM (eV)	DXRD FWHM (arcsec)
$x = 0.00$	GaAs	0.0673	0.123	1.509	4.58	
$x = 0.11$	GaAs	0.06276	0.28	1.3589	7.7	300
$x = 0.16$	GaAs	0.06032	0.49	1.305	10.37	400
$x = 0.20$	GaAs	0.05614	1.02	1.1965	18.3	430
$x = 0.31$	InP	no CR signal	no CR signal	0.975	68	1050
$x = 0.39$	InP	no CR signal	no CR signal	0.868	40.9	900
$x = 0.48$	InP	0.0435	0.47	0.825	4.7	40
$x = 0.53$	InP	0.04326	0.44	0.8036	3.27	30
$x = 0.59$	InP	0.0407	0.56	0.759	5.35	210
$x = 0.66$	InP	0.0392	0.45	0.7051	6.27	570
$x = 0.73$	InP	0.033	0.49			1030
$x = 0.82$	GaAs	0.0317	0.95			810
$x = 0.88$	GaAs	0.0301	0.68			730
$x = 0.93$	GaAs	0.0277	0.4			650
$x = 1.00$	GaAs	0.02453	0.094			350

ly interpolate the values of the dielectric constants ϵ_0 and the effective masses (m_e, m_{hh}, and m_{lh}) for GaAs and InAs, the binding energy E_d for each composition can be estimated. The energy band gap thus can be obtained by adding the binding energy to the peak position of the PL spectrum. The energy gap E_0 of $In_xGa_{1-x}As$ alloys as a function of alloy composition deduced from this measurement is shown in Fig. 2. In this figure we also show the fitting curves from previous reports.[12,13] We can see that most measured values agree well with the fitting curves, except for the data at $x=0.31$ and 0.39, which are smaller than the fitting results. The phenomenon that the PL position deviates to lower energy has also been reported by Dunstan *et al.*[14] They attributed this deviation to the existence of the recombination center related to the relaxation-induced $EL2$ defect. In our viewpoint, since the misfit dislocation density is rather high at the region of $x\sim0.3$ (see below), it is reasonable that the PL peak will shift to low energy due to the contributions coming from the deep defect- or impurity-related recombination. The compositional dependence of the FWHM of the PL spectra in $In_xGa_{1-x}As$ alloys is also plotted in Fig. 3. We found that the FWHM increases from $x=0$ to 0.31 and then decreases from $x=0.31$ to 0.53. As x exceeds 0.53, however, the FWHM increases slightly. The values of the PL peak position and FWHM are also listed in Table I. These data will be discussed again in later sections.

Let us now consider the results of the ODCR measurements. It is known that the ODCR signal is detected owing to the impact ionization of impurities or excitons via FIR-heated free carriers. Thus, at the resonance condition, when free carriers absorb most efficiently, the PL intensity is much effected. In our ODCR experiment, the spectrometer was fixed at the emission peak of the bound exciton as mentioned above. The ODCR spectra of the $In_xGa_{1-x}As$ alloys with $x\leq0.66$ are shown in Fig. 4. A clear CR signal can be observed when the changes of the PL intensity induced by FIR radiation are measured as a function of magnetic field. As x increases from 0 to 0.66,

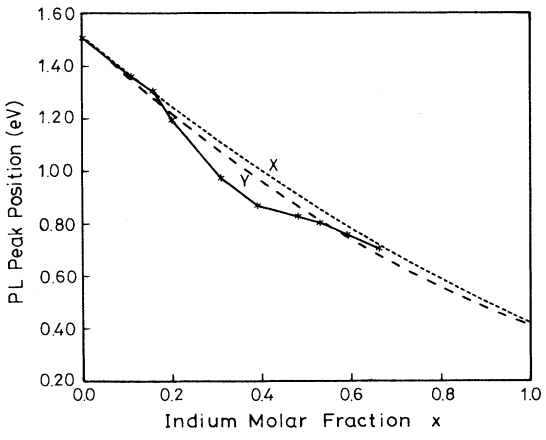

FIG. 2. Compositional dependence of the measured energy gap of $In_xGa_{1-x}As$ alloys (open squares). The dashed lines X and Y indicate the fitting curves of $0.32x^2-1.419x+1.519$ (Ref. 13) and $0.475x^2+0.6337x+0.4105$ (Ref. 12), respectively.

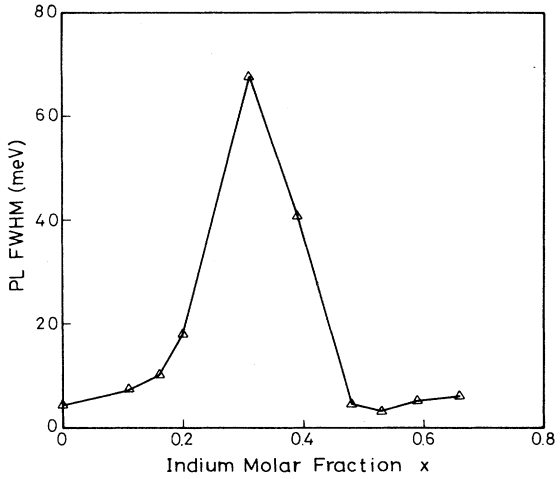

FIG. 3. Compositional dependence of the FWHM of CR on $In_xGa_{1-x}As$ alloys. The solid line is a guide for the eye.

the magnetic field of the CR position decreases. The signal at about 3 T for $x=0.48$ and 0.53 is assigned to the interimpurity transition of the residual donor, the $1s$-to-$2p^+$ transition.[15] The fact that interimpurity transition is not observed in other samples can be attributed to the linewidth broadening due to strong dislocation and/or impurity scatterings. The correlation between the linewidths of CR and the dislocation density obtained from DXRD measurement will be discussed in a later

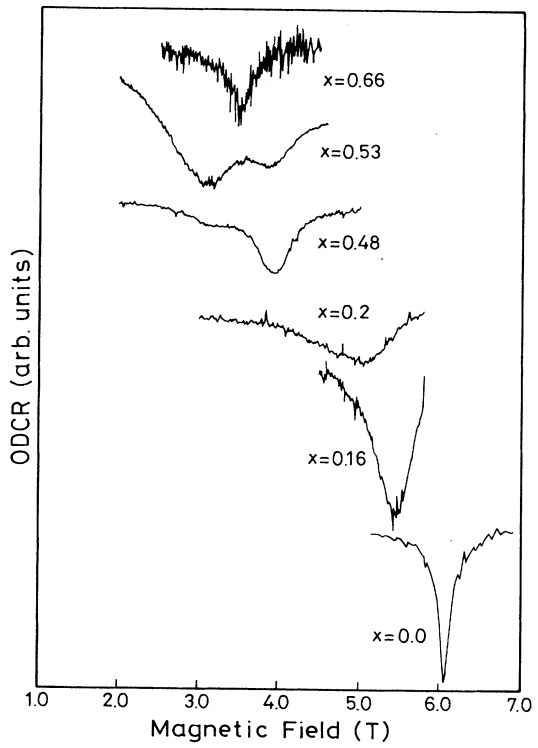

FIG. 4. The ODCR spectra of $In_xGa_{1-x}As$ alloys with $0\leq x\leq0.66$. $T=5$ K.

section. For the same reason, the fact that the CR signal disappears at $x=0.31$ and 0.39 can also be understood. The FIR-magnetophotoconductivity spectra for $In_xGa_{1-x}As$ alloys with $x \geq 0.73$ as a function of magnetic field are shown in Fig. 5. Similar to the trend as in the case of $x \leq 0.66$, the magnetic field of the resonant position decreases as x increases. At $x=1$, two peaks appear at the magnetic field of 1.93 and 2.25 T. The former can also be assigned to the $1s$-to-$2p^+$ interimpurity transition.[16]

From the position of the CR we can obtain the electron effective mass accurately. The compositional dependence of the effective mass m^* determined from Figs. 4 and 5 are collected in Fig. 6 (dots) and Table I. The experimental values ($x \leq 0.154$) reported by previous measurement are also shown in the same figure for comparison (squares). The best fit to our experimental results to the second-order term of x is plotted as the solid line. This empirical formula can be written as

$$m^*/m_0 = 0.009\,23x^2 - 0.0516x + 0.0675 \ . \quad (2)$$

For theoretical consideration, the treatment of the variation of the effective mass with alloy content in III-V compounds has been reported by Hermann and Weisbuch.[5] According to the $\mathbf{k}\cdot\mathbf{p}$ approximation, the effective mass can be obtained from the following expression:[5]

$$\frac{m_0}{m^*} - 1 = \frac{p^2}{3}\left[\frac{2}{E_0} + \frac{1}{E_0+\Delta_0}\right] - \frac{p'^2}{3}\left[\frac{2}{E(\Gamma_8^c)-E_0} + \frac{1}{E(\Gamma_7^c)-E_0}\right] + C \ , \quad (3)$$

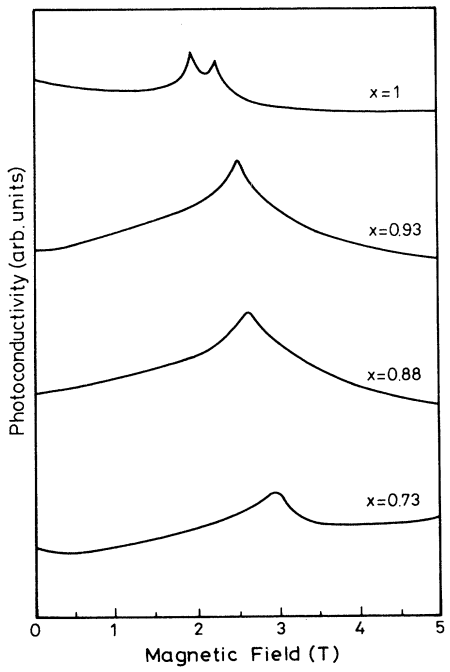

FIG. 5. FIR-magnetophotoconductivity spectra of $In_xGa_{1-x}As$ alloys with $0.73 \leq x \leq 1$. $T=5$ K.

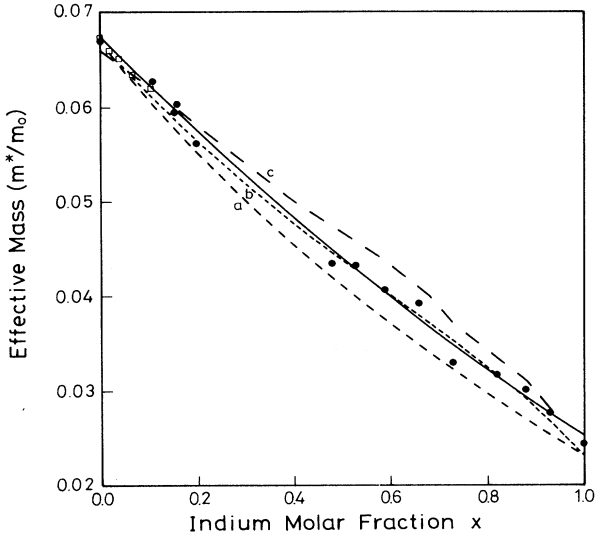

FIG. 6. Compositional dependence of the electron effective mass obtained from Figs. 4 and 5. The solid line is a fit to the data using the least-squares calculation. Curve *a* represents the result of a many-band $\mathbf{k}\cdot\mathbf{p}$ calculation using Eq. (3). Curve *b* represents the calculation using $\mathbf{k}\cdot\mathbf{p}$ theory, including the effect of alloy disorder. Curve *c* plots the result of tight-bonding calculation for comparison.

where Δ_0, p^2, p'^2, and C represent the spin-orbit splitting, the matrix element for the conduction–valence-band coupling, the matrix element describing the interaction of the Γ_6 conduction band with the Γ_5 conduction bands E_7 and E_8, and the constant ($C=-2$) used to approximate the residual influence of all other remaining bands, respectively. The band gap E_0 can be determined from the interpolation formula:[13] $1.519-1.419x+0.32x^2$. For Δ_0, p^2, p'^2, E_7, and E_8, we linearly interpolate the corresponding values for bulk GaAs and InAs.[17] In Fig. 6 (curve *a*) we show the calculated result of the compositional dependence of the effective mass using Eq. (3). Comparing with the experimental values, we find that the effective mass calculated from Eq. (3) is smaller than that obtained from measurements. This deviation has also been reported in the previous studies for several III-V compounds, such as $In_xGa_{1-x}As$ ($x \leq 0.154$), InP, GaAs, and $Ga_xIn_{1-x}As_yP_{1-y}$.[5,18–21]

The origin of this discrepancy may be attributed to the alloy disorder, which breaks the symmetry of the lattice and induces the mixing of the conduction and valence bands.[21–23] The conduction–valence-band mixing will lead to the transfer of valence-band states to the conduction band, thus increasing the effective mass in the conduction band.[22] This mixing effect is to reduce the p^2 in the $\mathbf{k}\cdot\mathbf{p}$ theoretical expression. Merian and Bhattacharjee suggested that the reduction of p^2 caused by the alloy disorder can be described by the factor $(1-f)$, where f is the band-mixing fraction.[23] The band-mixing fraction can be estimated by

$$f \sim x(1-x)\langle \delta V^2 \rangle / E_0^2 \ , \quad (4)$$

where $\langle \delta V^2 \rangle$ represents the potential fluctuations. The

strength of the fluctuations $\langle \delta V^2 \rangle$ has been roughly described by the random strain related to positional disorder[24] and the electronegativity difference related to chemical disorder.[22] For these two kinds of disorder, the dominant contribution to the band mixing is still not conclusive.[23] In our case, if we fit $\langle \delta V^2 \rangle$ as 0.18 eV^2, the compositional dependence of the effective mass will change from curve *a* to curve *b* as shown in Fig. 6. Under this consideration, our measurements can be explained very well. Thus, we may conclude that to analyze the electron effective mass in ternary alloys the conduction–valence-band mixing induced by the alloy disorder must be included. In Fig. 6, for comparison, we also show the theoretical result based on the tight-bonding formalism[25] (curve *c*), even though it cannot be used to describe our measurements. Further evidence for the effects of alloy disorder is illustrated in Fig. 7. In this figure the squares indicate the measured effective mass versus the measured energy gap, while the effective mass calculated by Eq. (3) is plotted using triangles. We can see that the difference between the measured and theoretical values increases as the energy gap decreases. This behavior can be accounted for by Eq. (4), which shows that the reduction of p^2 increases with decreasing energy gap. Thus, the correction in the effective mass using Eq. (3) also increases with decreasing energy gap, which will bring the theoretical values to coincide with the measured results.

The FWHM of the CR spectrum as a function of alloy composition in $In_xGa_{1-x}As$ alloys is plotted in Fig. 8. It shows two local maximums at $x = 0.2$ and 0.82. In order to probe the possible scattering mechanism for the variation of the CR linewidth, the samples investigated by the CR and PL measurements have also been studied by DXRD experiment. Figure 9 displays the FWHM of the (400) DXRD signals in our $In_xGa_{1-x}As$ alloys. If we compare Fig. 9 with Figs. 3 and 8, we find a strong correlation of the compositional dependence of FWHM's among these three measurements. Since the FWHM of the DXRD signal is very sensitive to the misfit and threading dislocations in heteroepitaxial systems, we thus conclude that the dominant scattering mechanism in $In_xGa_{1-x}As$ alloys is the dislocation scattering. It is known that there is a small environment which can provide the study of the dislocation scattering systematically. Our experiments, however, prove that the $In_xGa_{1-x}As$ system is a good candidate for this purpose.

It is known that the lattice of the $In_xGa_{1-x}As$ alloy matches with that of InP when $x = 0.53$. In Figs. 3 and 8 we can see that the FWHM's of the PL and CR spectra in the region of $0.3 \leq x \leq 0.53$ are much larger than those in the region of $0.53 \leq x \leq 0.75$. This means that the quality of the materials is quite different between the positive ($x > 0.53$) and negative ($x < 0.53$) mismatch systems. This phenomenon can be understood by studies reported recently.[25,26] It was found that the Ga concentrations as well as the cation disorder also play important roles in the initial growth stage. Because the gallium atom has a shorter surface migration length than that of the indium atom, the gallium atom can easily become a

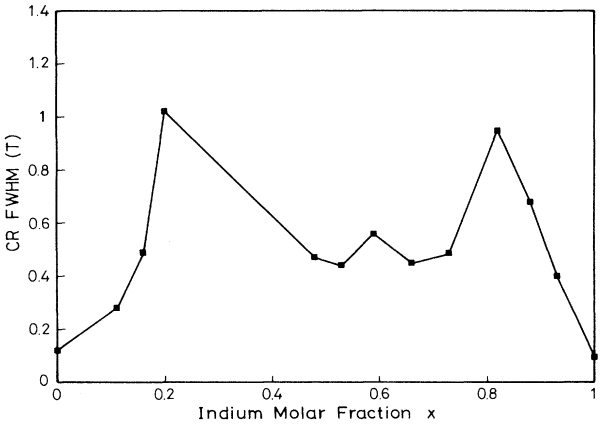

FIG. 8. Compositional dependence of the FWHM of cyclotron resonance in $In_xGa_{1-x}As$ alloys. The solid line is a guide for the eye.

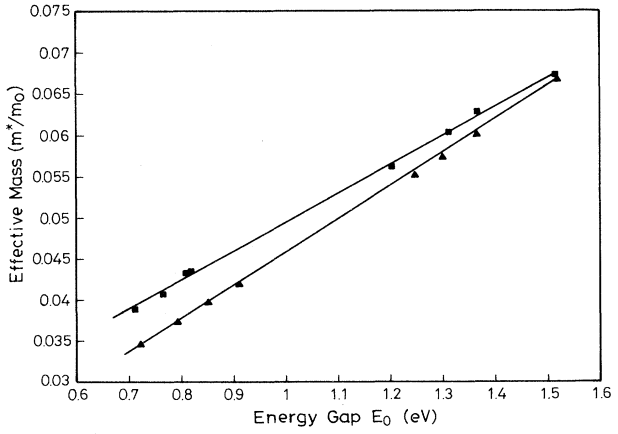

FIG. 7. Effective mass vs energy gap of $In_xGa_{1-x}As$ alloys with $0.66 \leq x \leq 1$. The squares and triangles indicate the experimental and calculated values, respectively. The solid lines are a guide for the eye.

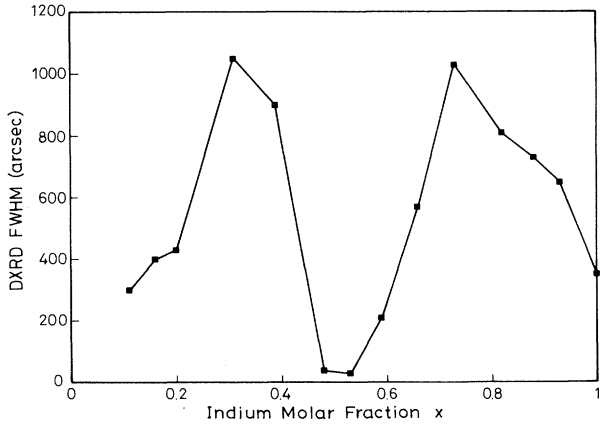

FIG. 9. FWHM of (400) DXRD signals for $In_xGa_{1-x}As$ alloys. The solid line is a guide for the eye.

heterogeneous nucleation center for island formation during the initial growth process. As a result, the strain field is incorporated into the high-density island coalescence process and causes the poor quality of the materials. Hence, except for the lattice mismatch, the surface migration lengths of cation atoms will also contribute to the determination of the quality of $In_xGa_{1-x}As$ epilayers. This behavior thus leads to the observation of the different properties between the positive and negative mismatch materials in our experiment.

IV. CONCLUSION

In conclusion, we have performed the CR and PL measurements of $In_xGa_{1-x}As$ alloys with $0 \leq x \leq 1$. The electron effective mass over a wide range of x has been accurately determined. Based on the five-band $\mathbf{k}\cdot\mathbf{p}$ calculation, the electron effective mass as a function of alloy composition has been analyzed. It is found that the calculated values are smaller than the experimental data. We point out that the effect of alloy disorder must be included in the analysis of the effective mass for ternary alloys. From the investigation of the linewidths of PL and CR spectra, we show that the FWHM's in these two measurements are strongly correlated with that of DXRD measurement. It indicates that the CR and PL signals are dominated by the dislocation scattering in $In_xGa_{1-x}As$ alloys. Additionally, we demonstrate that the lattice mismatch is not the only factor determining the quality of epilayers; surface migration lengths of cation atoms in the initial growth stage also play a very important role.

ACKNOWLEDGMENTS

This work was partly supported by the National Science Council of the Republic of China under Grant Contract No. NSC 84-2112-M-002-019.

[1]E. F. Hockings, I. Kudman, T. E. Seidel, C. M. Smelz, and E. F. Steigmeier, J. Appl. Phys. **37**, 2879 (1966).
[2]Yu. M. Burdukov, Yu. V. Mal'tsev, G. I. Pichakhchi, Yu. I. Ukhanov, and Kh. A. Khalikov, Fiz. Tekh. Poluprovodn. **4**, 1390 (1970) [Sov. Phys. Semicond. **4**, 1184 (1971)].
[3]M. B. Thomas and J. C. Woolley, Can. J. Phys. **49**, 2052 (1971).
[4]H. Fetterman, J. Waldman, and C. M. Wolfe, Solid State Commun. **11**, 375 (1972).
[5]C. Hermann and C. Weisbush, Phys. Rev. B **15**, 823 (1977).
[6]J. L. Shen, I. M. Chang, Y. M. Shu, Y. F. Chen, S. Z. Chang, and S. C. Lee, Phys. Rev. B **50**, 1678 (1994).
[7]P. G. Baranov, Yu. P. Veshchunov, R. A. Zhitnikov, N. G. Romanov, and Yu. G. Shreater, Pis'ma Zh. Eksp. Teor. Fiz. **26**, 369 (1977) [JETP Lett. **26**, 249 (1977)].
[8]M. G. Wright, N. Ahmed, A. Koohian, K. Mitchell, G. R. Johnson, B. C. Cavenett, C. R. Pidgeon, C. R. Stanley, and A. H. Kean, Semicond. Sci. Technol. **5**, 438 (1990).
[9]C. Wetzel, B. K. Meyer, and P. Omling, Phys. Rev. B **47**, 15 588 (1993).
[10]V. Swaminathan, R. A. Stall, A. T. Macrander, and R. J. Wunder, J. Vac. Sci. Technol. B **3**, 1631 (1985).
[11]A. P. Roth, M. A. Sacilotti, R. A. Masut, D. Morris, J. Young, and C. Lacelle, E. Fortin, and J. L. Brebner, Can. J. Phys. **67**, 330 (1989).
[12]K. H. Goetz, D. Bimberg, H. Jürgensen, J. Selders, A. V. Solomonov, G. F. Glinskii, and M. Razeghi, J. Appl. Phys. **54**, 4543 (1983).
[13]G. Hendorfer and J. Schneider, Semicond. Sci. Technol. **6**, 595 (1991).
[14]D. J. Dunstan, R. H. Dixon, P. Kidd, L. K. Howard, V. A. Wilkinson, J. D. Lambkin, C. Jeynes, M. P. Halsall, D. Lancefield, M. T. Emeny, P. J. Goodhew, K. P. Homewood, B. J. Sealy, and A. R. Adams, J. Cryst. Growth **126**, 589 (1993).
[15]S. Yamada, T. Fukui, K. Tsubaki, and A. Sugimura, Phys. Rev. B **32**, 8078 (1992).
[16]P. D. Wang, S. N. Holmes, T. Le, R. A. Stadling, I. T. Ferguson, and A. G. de Oliveira, Semicond. Sci. Technol. **7**, 767 (1992).
[17]*Intrinsic Properties of Group IV Elements and III-V, II-VI and I-VII Compounds,* edited by O. Madelung, M. Schulz, and H. Weiss, Landolt-Börnstein, New Series, Group III, Vol. 22, Pt. a (Springer-Verlag, New York, 1987).
[18]J. M. Chamberlain, A. A. Reeder, R. J. Turner, E. Kuphal, and J. L. Benchimol, Solid State Electron. **30**, 217 (1987).
[19]L. G. Shantharama, R. J. Nicholas, A. R. Adams, and C. K. Sarkar, J. Phys. C **18**, L443 (1985).
[20]R. J. Nicholas, J. C. Portal, C. Houlbert, P. Perrier, and T. P. Pearsall, Appl. Phys. Lett. **34**, 492 (1979).
[21]L. G. Shantharama, A. R. Adams, C. N. Ahmad, and R. J. Nicholas, J. Phys. C **17**, 4429 (1984).
[22]O. Berolo, J. C. Woolley, and J. A. Van Vechten, Phys. Rev. B **8**, 3794 (1973).
[23]M. Merian and A. K. Bhattacharjee, Solid State Commun. **55**, 1071 (1985).
[24]E. D. Siggia, Phys. Rev. B **10**, 5174 (1974).
[25]M. Jaffe and J. Singh, J. Appl. Phys. **65**, 329 (1989).
[26]S. Z. Chang, T. C. Chang, J. L. Shen, S. C. Lee, and Y. F. Chen, J. Appl. Phys. **74**, 6912 (1993).
[27]S. Z. Chang, S. C. Lee, C. R. Chen, and L. J. Chen, J. Appl. Phys. **75**, 1511 (1994).